JACS
JOURNAL OF THE AMERICAN CHEMICAL SOCIETY

Communication

pubs.acs.org/JACS

Resonance Raman Spectroscopy on [NiFe] Hydrogenase Provides Structural Insights into Catalytic Intermediates and Reactions

Marius Horch, Janna Schoknecht, Maria Andrea Mroginski, Oliver Lenz, Peter Hildebrandt,* and Ingo Zebger*

Institut für Chemie, Sekr. PC14, Technische Universität Berlin, Strasse des 17. Juni 135, D-10623 Berlin, Germany

Supporting Information

ABSTRACT: [NiFe] hydrogenases catalyze the reversible cleavage of hydrogen and, thus, represent model systems for the investigation and exploitation of emission-free energy conversion processes. Valuable information on the underlying molecular mechanisms can be obtained by spectroscopic techniques that monitor individual catalytic intermediates. Here, we employed resonance Raman spectroscopy and extended it to the entire binuclear active site of an oxygen-tolerant [NiFe] hydrogenase by probing the metal−ligand modes of both the Fe and, for the first time, the Ni ion. Supported by theoretical methods, this approach allowed for monitoring H-transfer from the active site and revealed novel insights into the so far unknown structure and electronic configuration of the hydrogen-binding intermediate of the catalytic cycle, thereby providing key information about catalytic intermediates and reactions of biological hydrogen activation.

The catalytic transformation of hydrogen by [NiFe] hydrogenases takes place at a heterobimetallic center (Figure 1), in which a Ni and an Fe ion are bridged by two cysteines.[1] Two further cysteines serve as terminal ligands to the Ni while the Fe is coordinated by additional diatomic ligands, one CO and two CN^-. Spectroscopic techniques are indispensable tools for elucidating the ground state conformation and electronic configuration of the catalytic intermediates, which is a prerequisite for the detailed understanding of the molecular mechanism. Previous spectroscopic studies on hydrogenases were primarily based on infrared (IR) and electron paramagnetic resonance (EPR) techniques, and only recently we have demonstrated that resonance Raman (RR) spectroscopy can provide complementary information on the active site structure.[2] However, the first RR spectroscopic study was restricted to the photoproduct of the reduced catalytic intermediates of the membrane-bound hydrogenase from *Ralstonia eutropha* (MBH). In the present study we extended this approach to different redox states, using the regulatory hydrogenase (RH) from the same organism. The RH represents a particularly convenient model system as it comprises the catalytic center and a relatively simple electron relay of three $[4Fe4S]^{1+/2+}$ clusters (Figure 1).[1] Compared to the MBH, this leads to less pronounced interference of the cluster-derived RR bands with those of the active site. In vivo, the RH acts as a sensor for H_2-mediated hydrogenase gene transcription, and consequently this enzyme displays a restricted number of active site redox states as compared to most other [NiFe] hydrogenases. Thus, each of these catalytically relevant states can be easily enriched for a detailed spectroscopic characterization.[3]

At room temperature, the oxidized RH occurs in the Ni_a−S state while the hydrogen-reduced enzyme persists in the hydride-containing Ni_a−C state (Figure 1). This is demonstrated by the state-specific sets of three IR bands corresponding to one CO and two CN stretching modes (Figure 1A,B). On the basis of EPR studies,[4] the hydride-containing Ni_a−C state was shown to (photo)convert to another potential catalytic intermediate termed Ni−L that can be trapped at temperatures below 100 K (Figure 1). The EPR-silent Ni_a−S species[3] is characterized by a vacant coordination site between Ni and Fe and, thus, assumed to serve as the initial hydrogen binding state.[1,5]

Upon excitation at 458 nm, RR spectra are obtained for the (as-isolated) oxidized and H_2-reduced RH at 80 K (Figure 1C,E). Intense signals below 400 cm^{-1} that are mainly due to $[4Fe4S]^{2+}$ clusters[6] are strongly diminished upon H_2-incubation, indicating reduction to the paramagnetic $[4Fe4S]^{1+}$ state, which is RR-silent due to decreased S → Fe charge transfer (CT) probabilities. Remarkably, reduction of these FeS clusters could not be monitored in previous EPR studies,[4] which can be explained by high spin ground states or very fast spin relaxation. Further distinct signals in the 400−600 cm^{-1} range of the RR spectrum predominantly reflect stretching and bending vibrations of the $Fe^{2+}(CO)(CN^-)_2$ moiety of the active site.[2] In contrast to our studies on the MBH, where the oxidized Ni_r−B state was RR-silent, characteristic fingerprints of the [NiFe] center are observed both for the as-isolated and the H_2-reduced RH. To circumvent interference with FeS cluster-derived RR bands, particularly in the oxidized state, excitation wavelengths (488 and 568 nm) more distant to the absorbance maximum of the S → Fe CT transition were employed (Figure 1D,F). These RR spectra are now dominated by the bands above 400 cm^{-1}, confirming their assignment to the RH active site. Changing the excitation wavelength also alters relative band intensities, thereby revealing additional bands. In this respect, further signals around 600 (and 450) cm^{-1} are best observed at 488 and 514 nm for the reduced and oxidized state, respectively (Figure 1D,F). Despite overall similarity of the band patterns, signals

Received: May 22, 2014
Published: June 23, 2014

   dx.doi.org/10.1021/ja505119q | *J. Am. Chem. Soc.* 2014, 136, 9870−9873

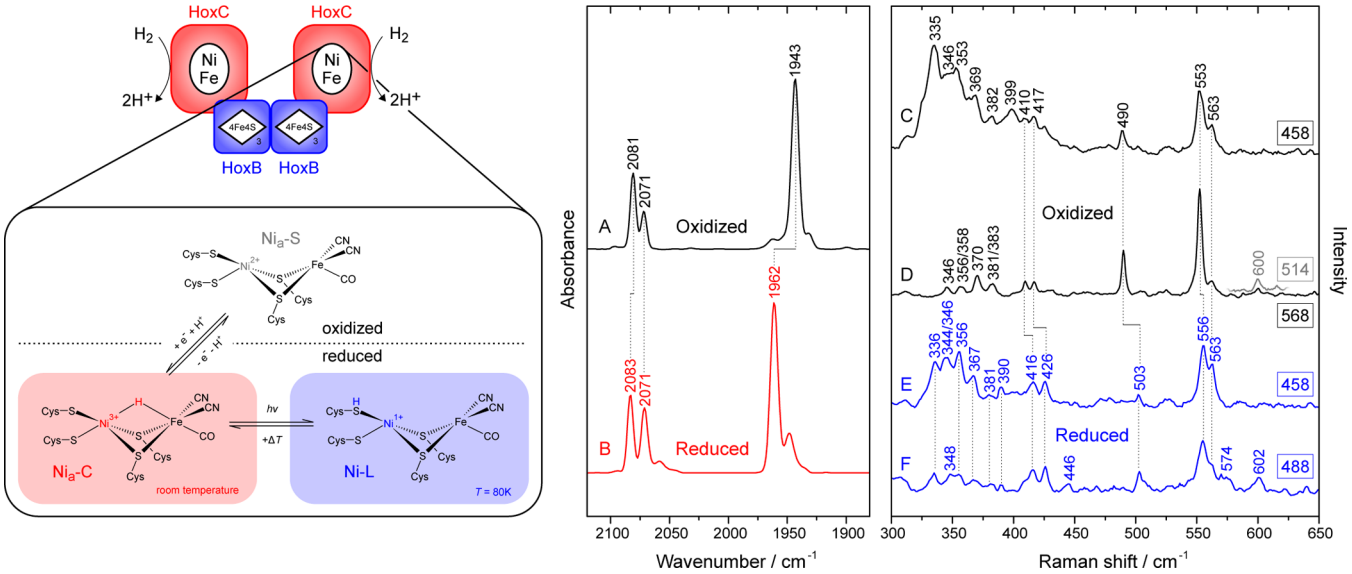

Figure 1. (Left) Overall subunit composition of the RH and structures of its active site in the main redox states. (Middle) Ambient temperature (283 K) IR spectra showing the region of ligand stretching modes (CO: 1900−1980 cm^{-1}; CN: 2040−2100 cm^{-1}) of the active site for as-isolated (A) and H_2-reduced RH (B). Spectra were normalized with respect to the CO stretching bands. (Right) Low temperature (80 K) RR spectra of as-isolated (C,D) and H_2-reduced RH (E,F), recorded with 458 (C,E), 488 (F), and 568 (514) nm (D) excitation. Spectra were normalized with respect to the band doublet around 560 cm^{-1}.

from the oxidized and reduced active site can be clearly distinguished by differences in the band positions (up to 13 cm^{-1}). This shows that different [NiFe] redox states can be selectively probed, identified, and characterized by RR spectroscopy (see Table SI 5 for a list of all observed RR bands).

While the oxidized state of the RH can be readily assigned to Ni_a−S, the reduced one may either correspond to Ni_a−C or the photoproduct Ni−L, since Ni_a−C → Ni−L photoconversion may be readily induced by the RR probe beam at 80 K.[2,4] To discriminate between the two states, the RH was reduced either with H_2 or D_2 in order to scan for H/D-sensitive metal−hydride vibrations expected for the Ni_a−C state (Figure 1). Adopting a previously established quantum mechanical (QM) model of the active site,[7,8] Ni−H/D−Fe stretching frequencies of 1250/888 cm^{-1} were calculated. However, no H/D sensitive bands could be observed experimentally in the typical range for bridging metal hydrides (800−1600 cm^{-1}).[9] As this negative result might be caused by low resonance enhancement or large band broadening,[9,10] we also considered minor contributions of metal-hydride coordinates to the RR-active modes between 400 and 600 cm^{-1} that are dominated by the Fe-ligand stretching and bending coordinates.[2] According to QM calculations (Table SI 6) and in line with a recent RR spectroscopic investigation of a [NiFe] model compound,[10] such contributions would give rise to H/D shifts of up to 8 cm^{-1}. However, the experimental spectra of H_2- and D_2-reduced RH are identical (Figure SI 7). Therefore, we conclude that RR spectroscopy probes specifically the Ni−L state of the reduced RH, which confirms previous observations for the MBH.[2] Ni−H bond dissociation upon Ni_a−C photoconversion was previously demonstrated by EPR spectroscopy,[4] and this observation has been generally interpreted as a removal of the bridging hydride. Notably, H/D insensitivity of Fe-centered modes of Ni−L provides the first experimental evidence for Fe−H bond dissociation, thereby verifying the proposed H-transfer from the bridging position of the active site. This conclusion is also supported by the absence of a terminal Fe−H stretching vibration in the 1700−2300 cm^{-1} region of low-temperature IR spectra recorded from the Ni−L state of the *Re* MBH.[2,9]

For a comprehensive assignment and analysis of the observed RR bands, vibrational frequencies were calculated for several structural variants of the Ni−L and Ni_a−S states (Figures 2 and SI 8). Because of the lack of a three-dimensional structure of the RH, these calculations were restricted to a pure quantum mechanical model of the active site (SI 4). Nonetheless, these calculations reproduce the overall band pattern and the experimental frequencies of both redox states quite well (Figure SI 8). Furthermore, the reliability of this computational approach can be assessed by comparison of calculated modes with the experimental spectrum of the reduced MBH, which was shown to represent the Ni−L state presumably containing a protonated terminal cysteine.[2] Here, calculated frequencies from the QM model agree within ±15 cm^{-1} (average error ±6 cm^{-1}). This margin is comparable to the intrinsic accuracy of the method and results obtained from a quantum mechanical/molecular mechanical (QM/MM) model that took into account effects of the MBH protein environment (Table SI 9). The most notable deviation refers to the Fe−CO stretching mode, which is systematically overestimated. Nevertheless, this mode may serve as a valuable spectral marker for structural and electronic variations of the [NiFe] center if one takes into account that, in contrast to the absolute values, frequency shifts are predicted with relatively high confidence. This is also indicated by very similar values for experimental (MBH) and calculated (QM and QM/MM) ^{13}C isotopic shifts of Ni−L (Table SI 9).

While the oxidized state of the RH can be unambiguously assigned to Ni_a−S, the Ni electronic ground state and geometry of this EPR-silent catalytic intermediate remained so far ambiguous (Figure 2). This ambiguity is a major challenge for the understanding of biological hydrogen activation, as these

dx.doi.org/10.1021/ja505119q | J. Am. Chem. Soc. 2014, 136, 9870−9873

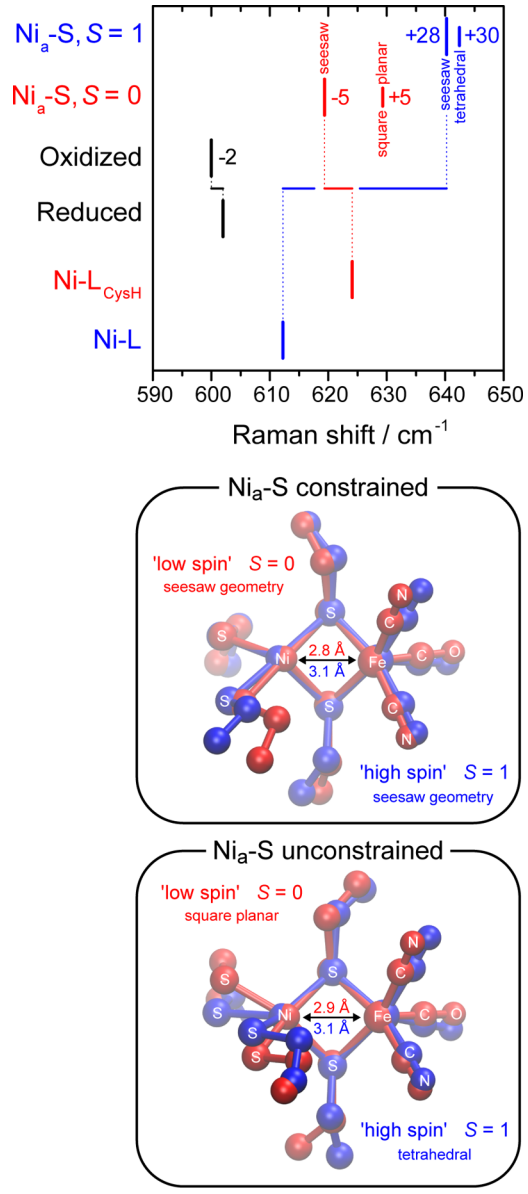

Figure 2. (Top) Experimental band positions of as-isolated and H_2-reduced RH (black) compared with calculated Fe−CO stretching frequencies obtained for structural variants of the Ni_a−S and Ni−L redox states (red, blue). (Bottom) Structural and electronic variants of Ni_a−S. Hydrogen atoms are not shown.

structural factors represent key determinants for the process of hydrogen binding to the active site.[5]

In principle, Ni_a−S could exhibit a distorted square planar (S = 0), tetrahedral (S = 1), or seesaw Ni geometry (S = 0 or S = 1).[5] In the experimental spectra, the Fe−CO stretching frequency is nearly the same for Ni_a−S and Ni−L ($\Delta\nu$ = −2 cm^{-1}). This observation is well reproduced by the calculations, assuming an S = 0 ground state for Ni_a−S and a single protonated cysteine ligand for Ni−L (Figure 2). While a square planar geometry ($\Delta\nu$ = +5 cm^{-1}) cannot be entirely ruled out within the accuracy of the theoretical method, comparison with the experimental data clearly favors a seesaw geometry with constrained S−Ni−S angles ($\Delta\nu$ = −5 cm^{-1}). In contrast, a high spin configuration (S = 1) for Ni_a−S or four thiolates in Ni−L result in Fe−CO stretching frequencies that differ by up to +30 cm^{-1}.

From this point of view, RR spectroscopy clearly favors a singlet rather than a triplet ground state for Ni_a−S. Interestingly, this conclusion is independent of the Ni coordination geometry, but related to the Ni−Fe distance, which is shorter for the low spin configuration (Figure 2). This is due to the higher acidity of low spin Ni^{2+} toward donor ligands, which may account for the lower Fe−CO stretching frequency as well as the higher H_2 binding capability[5] of the singlet form. Moreover, the shorter Ni−Fe distance likely reduces the reorganization energy associated with hydride binding, thereby accelerating an important reaction step in the catalytic cycle. Notably, a very recent theoretic study concluded that efficient hydrogen binding is only possible in a scenario, where the active site exhibits a low spin Ni^{2+} ion in a distorted seesaw geometry.[5] In fact, the present work provides the first experimental confirmation of this structural hypothesis.

While the Fe site of hydrogenase is well probed by the Fe−CO/CN modes discussed above, metal−ligand modes involving Ni−S coordinates were so far spectroscopically inaccessible. This situation represents a major challenge since these modes may provide valuable information, especially for [NiFe] active site intermediates that are EPR-silent or inappropriate for RR monitoring of Fe−CO/CN vibrations. For the Ni−L state (Ni^{1+}), S → Ni CT transitions are expected to be very weak, resulting in extremely low resonance enhancement that per se impairs the detection of these modes in the RR spectrum. In contrast, CT probabilities may be higher for Ni_a−S (Ni^{2+}) as also indicated by the RR spectroscopic detection of Ni−S modes in biological and synthetic Ni^{2+} tetrathiolates.[11] Appearing between 250 and 400 cm^{-1}, these modes overlap with the more intense RR bands of oxidized FeS clusters in hydrogenase. Therefore, we applied 568 nm excitation to keep contributions from the FeS cofactors low (vide supra, Figure SI 11). The resulting vibrational manifold displayed in this spectral range (Figure 3) can be attributed to modes involving Ni−S and Fe−S coordinates as well as cysteine side chain coordinates of the active site, which is in line with predictions from the QM calculations. This conclusion was confirmed experimentally by comparison of RR spectra obtained from RH preparations containing either ^{64}Ni or ^{58}Ni (Figures 3 and SI 12). Small but clearly detectable

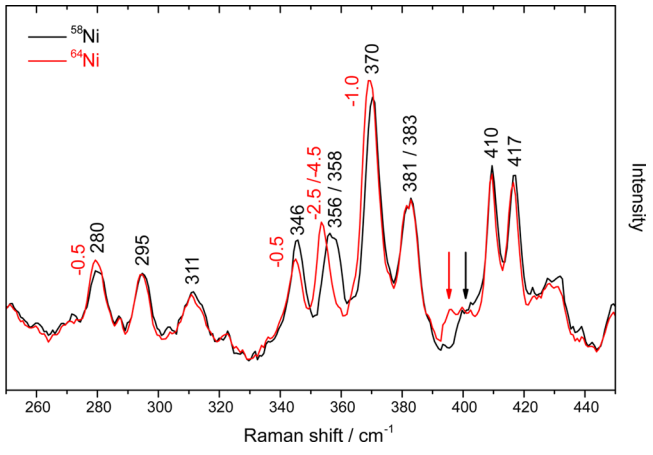

Figure 3. Low temperature (80 K) RR spectra of as-isolated ^{58}Ni (black) and ^{64}Ni (red) containing RH, recorded with 568 nm excitation. Apparent isotopic shifts, as observed under the present experimental conditions, are indicated by negative numbers. Regions with pronounced but unresolved isotope effects are marked by arrows.

dx.doi.org/10.1021/ja505119q | J. Am. Chem. Soc. 2014, 136, 9870−9873

frequency shifts between 1 and 5 cm^{-1} were found for several bands between 340 and 380 cm^{-1} reflecting the involvement of Ni−S stretching coordinates in agreement with the QM calculations.

In the present study we have demonstrated that RR spectroscopy can selectively probe the vibrational signature of the active site in different, catalytically active redox states, including Fe−ligand and, as shown here for the first time, Ni−ligand modes. This approach relies on the appropriate choice of excitation wavelengths allowing resonance enhancement via weak CT transitions and limiting interference from FeS cluster signals. In this sense, the methodology may also be beneficial for the characterization of other multicofactor enzymes. For Fe-ligand modes of [NiFe] hydrogenases, enhancement appears to be restricted to intermediates with a five-coordinate Fe site, allowing for the identification of redox states with a vacant coordination site between Ni and Fe. In combination with QM calculations, valuable information on the electronic and structural properties of the active site can be extracted from these metal−ligand modes. In this respect, the present approach allowed for the assignment of the electronic configuration and geometry of the hydrogen-binding Ni_a−S intermediate and the first observation of Fe−H bond dissociation during Ni_a−C → Ni−L photoconversion. In this way, RR spectroscopy complements EPR and IR techniques as an important tool for characterizing active site intermediates of hydrogenases, also in those cases where protein structural models are not available.

■ ASSOCIATED CONTENT

Supporting Information

SI 1−4: Description of experimental and computational details. SI 5−12: Complementary spectroscopic and theoretical data. This material is available free of charge via the Internet at http://pubs.acs.org.

■ AUTHOR INFORMATION

Corresponding Authors

hildebrandt@chem.tu-berlin.de
ingo.zebger@tu-berlin.de

Notes

The authors declare no competing financial interest.

■ ACKNOWLEDGMENTS

The work was supported by the DFG (Cluster of Excellence UniCat), and the Senate of Berlin ("Nachhaltige Chemie").

■ REFERENCES

(1) Shafaat, H. S.; Rudiger, O.; Ogata, H.; Lubitz, W. *Biochim. Biophys. Acta* **2013**, *1827*, 986−1002.

(2) Siebert, E.; Horch, M.; Rippers, Y.; Fritsch, J.; Frielingsdorf, S.; Lenz, O.; Velazquez, E. F.; Siebert, F.; Paasche, L.; Kuhlmann, U.; Lendzian, F.; Mroginski, M. A.; Zebger, I.; Hildebrandt, P. *Angew. Chem., Int. Ed. Engl.* **2013**, *52*, 5162−5165.

(3) Bernhard, M.; Buhrke, T.; Bleijlevens, B.; De Lacey, A. L.; Fernandez, V. M.; Albracht, S. P.; Friedrich, B. *J. Biol. Chem.* **2001**, *276*, 15592−15597.

(4) Brecht, M.; van, G. M.; Buhrke, T.; Friedrich, B.; Lubitz, W. *J. Am. Chem. Soc.* **2003**, *125*, 13075−13083.

(5) Bruschi, M.; Tiberti, M.; Guerra, A.; De Gioia, L. *J. Am. Chem. Soc.* **2014**, *136*, 1803−1814.

(6) Czernuszewicz, R. S.; Macor, K. A.; Johnson, M. K.; Gewirth, A.; Spiro, T. G. *J. Am. Chem. Soc.* **1987**, *109*, 7178−7187.

(7) Horch, M.; Rippers, Y.; Mroginski, M. A.; Hildebrandt, P.; Zebger, I. *ChemPhysChem* **2013**, *14*, 185−191.

(8) Rippers, Y.; Horch, M.; Hildebrandt, P.; Zebger, I.; Mroginski, M. A. *ChemPhysChem* **2012**, *13*, 3852−3856.

(9) Nakamoto, K. *Infrared and Raman Spectra of Inorganic and Coordination Compounds—Applications in Coordination, Organometallic, and Bioinorganic Chemistry*, 6th ed.; John Wiley and Sons, Inc.: Hoboken, NJ, 2009.

(10) Shafaat, H. S.; Weber, K.; Petrenko, T.; Neese, F.; Lubitz, W. *Inorg. Chem.* **2012**, *51*, 11787−11797.

(11) Huang, Y. H.; Moura, I.; Moura, J. J. G.; LeGall, J.; Park, J. B.; Adams, M. W. W.; Johnson, M. K. *Inorg. Chem.* **1993**, *32*, 406−412.